NANO LETTERS

Letter

pubs.acs.org/NanoLett

Growth of Large-Area and Highly Crystalline MoS_2 Thin Layers on Insulating Substrates

Keng-Ku Liu,[†,&] Wenjing Zhang,[†,&] Yi-Hsien Lee,[†] Yu-Chuan Lin,[†] Mu-Tung Chang,[‡] Ching-Yuan Su,[§] Chia-Seng Chang,[‡] Hai Li,[∥] Yumeng Shi,[#] Hua Zhang,[∥] Chao-Sung Lai,[§] and Lain-Jong Li*[,†,⊥]

[†]Institute of Atomic and Molecular Sciences, Academia Sinica, Taipei 10617, Taiwan

[‡]Institute of Physics, Academia Sinica, Taipei 11529, Taiwan

[§]Department of Electronic Engineering, Chang Gung University, Tao-Yuan 333, Taiwan

[∥]School of Materials Science and Engineering, Nanyang Technological University, Singapore

[⊥]Department of Photonics, National Chiao Tung University, HsinChu 300, Taiwan

[#]Department of Electrical Engineering and Computer Sciences, Massachusetts Institute of Technology, Cambridge, Massachusetts 02139, United States

Supporting Information

ABSTRACT: The two-dimensional layer of molybdenum disulfide (MoS_2) has recently attracted much interest due to its direct-gap property and potential applications in optoelectronics and energy harvesting. However, the synthetic approach to obtain high-quality and large-area MoS_2 atomic thin layers is still rare. Here we report that the high-temperature annealing of a thermally decomposed ammonium thiomolybdate layer in the presence of sulfur can produce large-area MoS_2 thin layers with superior electrical performance on insulating substrates. Spectroscopic and microscopic results reveal that the synthesized MoS_2 sheets are highly crystalline. The electron mobility of the bottom-gate transistor devices made of the synthesized MoS_2 layer is comparable with those of the micromechanically exfoliated thin sheets from MoS_2 crystals. This synthetic approach is simple, scalable, and applicable to other transition metal dichalcogenides. Meanwhile, the obtained MoS_2 films are transferable to arbitrary substrates, providing great opportunities to make layered composites by stacking various atomically thin layers.

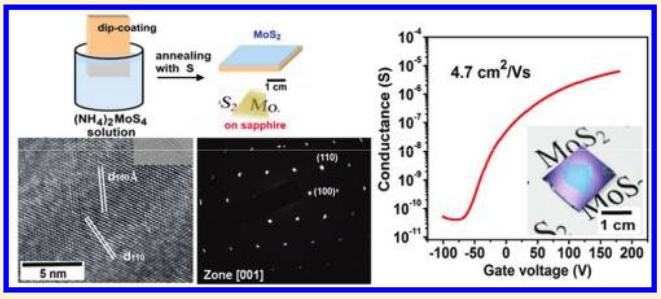

KEYWORDS: *Transition metal dichalcogenides, molybdenum disulfide, layered materials, transistors, two-dimensional materials, semiconductors*

Graphene holds great promises for replacing conventional Si semiconductors in applications such as high-frequency devices and biochemical sensors because of its extremely high carrier mobility and sensitivity to environmental charges.[1,2] However, the zero energy gap of graphene retards its application in logic electronics. Recently, transition metal dichalcogenides have attracted great attention owing to their two-dimensional (2-d) layer structure analogous to graphene. The transistors fabricated with the molybdenum disulfide (MoS_2) atomic thin layers exhibit excellent on/off current ratio and high carrier mobility, which make them suitable for next generation transistors.[3,4] Meanwhile, when the dimension of MoS_2 is reduced from a bulk form to a 2-d monolayer sheet, its optical properties change due to the transformation of the band gap from an indirect to a direct one.[5−11] Significant efforts have been devoted to prepare MoS_2 thin layers, including Scotch tape assisted micromechanical exfoliation,[3−5,12] intercalation assisted exfoliation,[13−20] solution exfoliation,[15,16,21−23] physical vapor deposition,[25,26] hydrothermal synthesis,[27] electrochemical synthesis,[28] sulfurization of molybdenum oxides,[29,30] and thermolysis of the precursor containing Mo and S atoms.[23] However, MoS_2 tends to form zero-dimensional closed structures (fullerene-like nanoparticles) or one-dimensional nanotube structures during the synthesis.[31] The method to synthesize large-area and high-quality MoS_2 sheets with good electrical performance is still rare. Thick MoS_2 films (>several tens of nanometers) have been prepared by spin-coating and thermolysis of alkyldiammonium thiomolybdate or ammonium thiomolybdate in polar organic solvents.[31−33] However, the carbon contaminations from the residual solvent molecules[32] were suspected to cause the sulfur deficit in the composition (stoichiometric ratio S/Mo < 2). The produced MoS_2 films are often amorphous or low-crystalline structures. Here, we report a two-step thermolysis process, which is able to grow highly crystalline and large-area MoS_2 thin sheets on a variety of

Received: December 10, 2011
Revised: February 16, 2012
Published: February 27, 2012

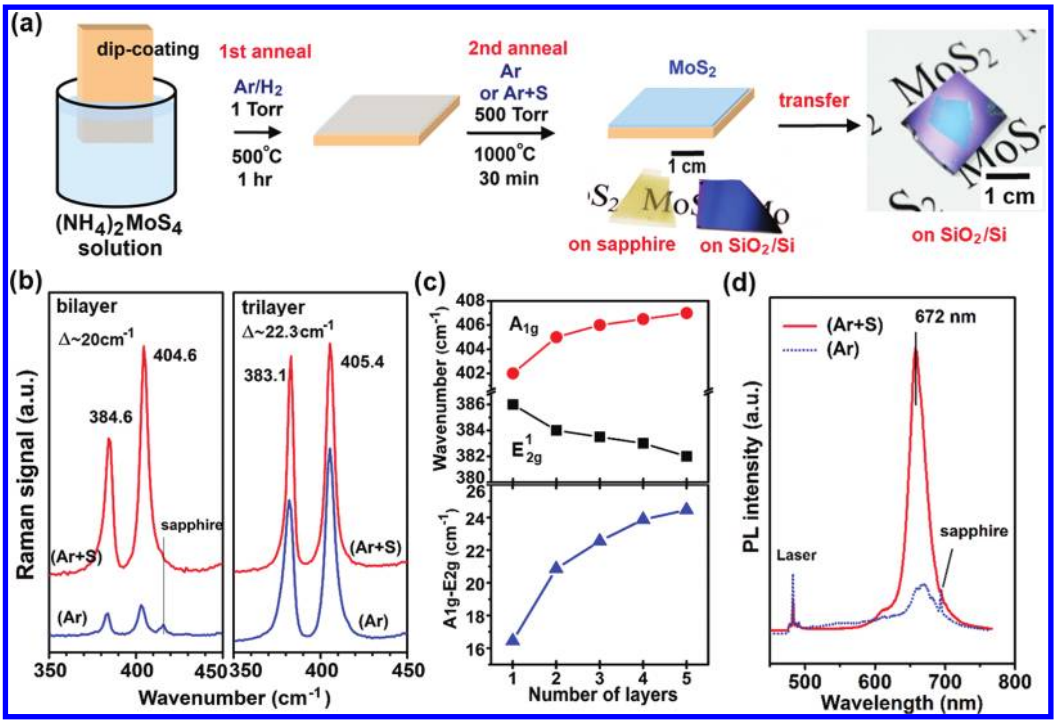

Figure 1. (a) Schematic illustration of the two-step thermolysis process for the synthesis of MoS_2 thin layers on insulating substrates. The precursor $(NH_4)_2MoS_4$ was dip-coated on SiO_2/Si or sapphire substrates followed by the two-step annealing process. The as-grown MoS_2 film can be transferred onto other arbitrary substrates. (b) Raman spectra for the bilayer and trilayer MoS_2 sheets grown on sapphire substrates (excitation laser: 473 nm), where the labels (Ar) and (Ar + S) represent the MoS_2 sheets separately prepared in pure Ar and in the mixture of Ar and sulfur during the second annealing. (c) Energies of the two characteristic Raman peaks for the micromechanically exfoliated MoS_2 films with various number of layers. The peak energy difference shown in the bottom graph can be used to identify the number of MoS_2 layers. (d) The PL intensity of the trilayer MoS_2 thin films prepared in (Ar + S) is stronger than those prepared in pure Ar (excitation laser 473 nm; spectra were normalized by Raman scattering peak at around 482 nm).

insulating substrates. Most importantly, the field-effect transistor (FET) devices based on these MoS_2 films exhibit high on/off current ratios and excellent carrier mobility values, comparable with those obtained from the micromechanical exfoliated MoS_2 thin sheets.

It has been reported that the thermolysis of ammonium thiomolybdates $(NH_4)_2MoS_4$ in an N_2 environment resulted in the conversion of $(NH_4)_2MoS_4$ to MoS_3 at 120−360 °C,[34] as shown in eq 1, and the conversion of MoS_3 to MoS_2 (eq 2) required the annealing at a higher temperature, for example, above 800 °C. It was also suggested that the conversion of $(NH_4)_2MoS_4$ to MoS_2 was further lowered to ∼425 °C in the presence of H_2 gas,[34] as described in eq 3.

$$(NH_4)_2MoS_4 \rightarrow 2NH_3 + H_2S + MoS_3 \quad (1)$$

$$MoS_3 \rightarrow MoS_2 + S \quad (2)$$

$$(NH_4)_2MoS_4 + H_2 \rightarrow 2NH_3 + 2H_2S + MoS_2 \quad (3)$$

To obtain high quality of MoS_2 thin film, it is rational to increase the thermolysis temperature. Note that the direct annealing of the $(NH_4)_2MoS_4$ film at 1000 °C in an inert gas does not produce good quality of MoS_2 likely due to that the transformation process of $(NH_4)_2MoS_4$ to MoS_2 involves many steps, and these steps may be easily affected by the presence of oxygen. Thus, H_2 gas is needed to avoid the oxidation. However, we also notice that the MoS_2 decomposes in H_2 when the temperature is higher than 500 °C. Thus, a two-step process is developed in this study.

Figure 1a schematically illustrates the two-step process for the synthesis of MoS_2 thin layers. High purity of $(NH_4)_2MoS_4$ (Alfa Aesar, purity of 99.99%; 0.25 g) was added to 20 mL of dimethylformamide (DMF) to form a 1.25 wt % solution. The solution was sonicated for 20 min before use. An insulating substrate such as sapphire or 300 nm SiO_2 on Si (SiO_2/Si) was first cleaned with a standard piranha solution (H_2SO_4/ H_2O_2 ∼ 7/3). After 10 min baking on a hot plate at 80 °C, the substrate was then immersed into the $(NH_4)_2MoS_4$ solution, followed by slow pulling (0.5 mm/s) to form a thin $(NH_4)_2MoS_4$ film. The substrate was then baked on a hot plate at 120 °C for 30 min. The annealing processes were performed in a homemade furnace system, where the sample in the quartz tube could be quickly moved between a hot zone (center of the furnace) and a cold zone using a magnet (Figure S1 in Supporting Information). The freshly prepared thin $(NH_4)_2MoS_4$ film was placed in the cold zone of the quartz tube flowing with a gas mixture (Ar/H_2 flow rate = 4/1; at 1 Torr). When the center of the furnace reached 500 °C, the substrate was moved to the hot zone of the furnace for the first annealing. The chamber was kept at a low pressure (1 Torr) in an Ar/H_2 atmosphere (flow rate 4:1) to efficiently remove the residual solvent, NH_3 molecules, and other byproducts dissociated from the precursors. Sixty minutes later, the sample was moved to the cold zone, and the gas environment was changed to Ar (or Ar + S) at 500 Torr. Then the sample is moved to the center of the furnace again for the second annealing when the hot zone reached 1000 °C. The film after the first annealing exhibits two characteristic MoS_2 Raman peaks (the E^1_{2g} mode at ∼382 and the A_{1g} mode at ∼405 cm^{-1}) as shown in Figure S2. It has been

dx.doi.org/10.1021/nl2043612 | Nano Lett. 2012, 12, 1538−1544

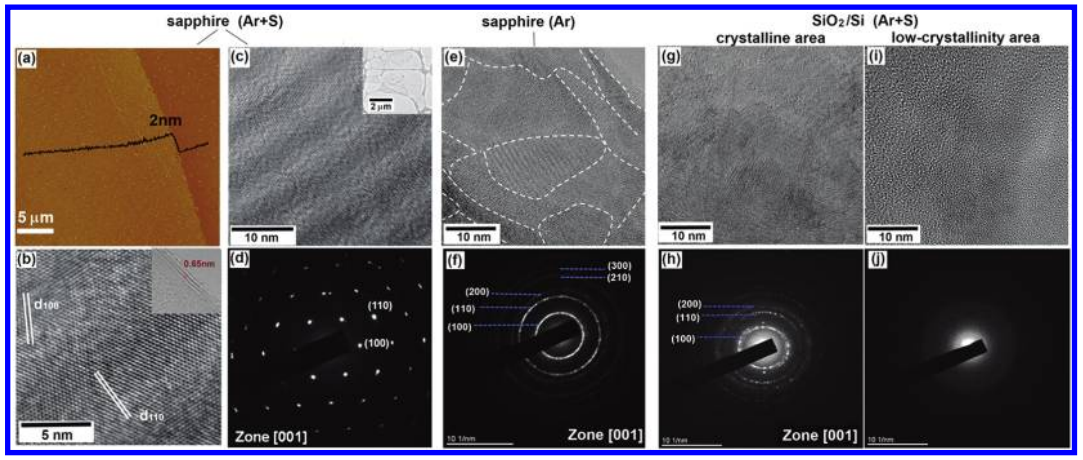

Figure 2. (a) AFM image of the MoS_2 trilayer grown on a sapphire substrate annealed with the presence of sulfur (Ar + S). (b) High-resolution TEM image for the MoS_2 trilayer. The *d*100 is 0.27 nm, and *d*110 is 0.16 nm. Inset is the TEM image of MoS_2 film edge, where three layers of MoS_2 are identified. (c) TEM image and (d) the SAED pattern of the MoS_2 trilayer sample discussed in (b). (e) TEM image and (f) the SAED pattern for the MoS_2 grown on sapphire with Ar annealing. (g, i) TEM images and (h, j) the SAED patterns for the MoS_2 trilayer grown on a SiO_2/Si substrate annealed with (Ar + S).

reported that the MoS_2 structure formed at the thermolysis temperature higher than 300 °C.[32,34] However, the relatively larger E^1_{2g} peak width (~10 cm^{-1}) and weaker intensity (relative to the substrate Si peak at 520 cm^{-1}) suggest that the crystal structure of MoS_2 is still not perfect. Note that the E^1_{2g} peak width for the MoS_2 layers obtained by micromechanical exfoliation is around 4−5 cm^{-1} (Figure S3). The samples after the first annealing are subjected to the 1000 °C annealing in pure Ar or in the mixture of Ar and sulfur. The sulfur can be used as a protection gas against the oxidation. Note that the sulfur is introduced into the chamber in a powder form, and the powders become sulfur vapors at the process temperature. As shown in Figure S2, the intensity of two characteristic Raman peaks significantly increases and the E^1_{2g} peak width narrows when the film is further subjected to the second annealing, indicating the high-temperature annealing at 1000 °C in Ar improves the MoS_2 crystal structure. Surprisingly, the addition of sulfur in the second annealing process greatly improved the crystallinity and electrical performance of the MoS_2 thin layers. These arguments are also supported by the photoluminescence (PL) and electrical measurements (conductivity vs gate voltage) for the MoS_2 layers directly formed on SiO_2/Si substrates after the first annealing and those subjected to the second annealing in pure Ar or in the environment with sulfur (Figure S2). It is also noted that the MoS_2 layer formed with only the first 500 °C annealing does not show any gate dependence (Figure S2).

The obtained MoS_2 films are uniform and continuous based on the optical micrograph shown in Figure 1a. In general, the more diluted precursor solution and faster dip-coating result in a thinner MoS_2 layer. Here, we aim at large-area and good quality film for electronic applications. The optimized process reported here is able to produce very homogeneous MoS_2 trilayers across the whole sample; however, MoS_2 bilayers are still occasionally found at some locations of the trilayer film. Figure 1b shows the Raman spectra for the trilayer MoS_2 sheets grown on sapphire substrates, where the labels (Ar) and (Ar + S) represent the MoS_2 sheets separately annealed in pure Ar and in the mixture of Ar and sulfur during the second annealing. The Raman spectra for the occasionally found MoS_2 bilayers are also shown. To compare the Raman signatures of synthesized and micromechanically exfoliated MoS_2 thin sheets, we have performed the Raman measurements for the micromechanically exfoliated MoS_2 thin sheets with various thickness (number of layers), where the Raman spectra are shown in Figure S3. Figure 1c shows the energies of the two characteristic Raman peaks for the exfoliated MoS_2 sheets. The energy difference between two Raman peaks (Δ) can be used to identify the number of MoS_2 layers,[8,15] and the relation is shown in the bottom curve of Figure 1c. The Δ value obtained in the left and right of Figure 1b is ~20 and ~22.3 cm^{-1}, respectively, corresponding to the bilayer and trilayer MoS_2 films based on the results in Figure 1c.

In addition to Raman features, we observe that photoluminescence (PL) is also very sensitive to the quality of the MoS_2 layers. The PL spectra in Figure 1d clearly show that the large-area MoS_2 trilayer annealed in the presence of sulfur exhibits a stronger PL intensity compared to that annealed in the environment without sulfur. Note that we have examined the MoS_2 films obtained at the temperature lower than 1000 °C such as 800, 900, and 950 °C during the second annealing. Our spectroscopic measurements suggest that the crystal structures of these films were poorer than that obtained at 1000 °C. The quality of MoS_2 layer is also determined by the substrate used for MoS_2 growth. We prepared the MoS_2 trilayers grown on sapphire and SiO_2/Si separately and then transfer both samples onto freshly cleaned SiO_2/Si substrates for spectroscopic measurements. The Raman and PL spectra in Figure S4 consistently show that the quality of the MoS_2 layers grown on sapphire is superior than that grown on SiO_2/Si. The electrical performance (electron mobility and on/off current ratio) shown in Figure S4 also strongly supports this conclusion. It is known that SiO_2 is less stable than sapphire at high temperature; thus, it is suspected that the oxygen from SiO_2 may react with the MoS_2 film, resulting in lower quality of MoS_2 layers. In general, the PL and Raman peak intensities may be used to indicate the crystalline quality of MoS_2 thin layers.

The atomic force microscope (AFM) topographic image in Figure 2a for the obtained trilayer MoS_2 film after the second annealing with the presence of sulfur reveals that the film is uniformly flat and with a thickness around 2 nm, where the measured thickness is in agreement with the reported value for

dx.doi.org/10.1021/nl2043612 | *Nano Lett.* 2012, 12, 1538−1544

exfoliated trilayer MoS_2.[3,8,35] The high-resolution tunneling electron microscopy (HRTEM) image in Figure 2b clearly reveals the periodic atom arrangement of the MoS_2 film at a selected location. The inset displays the low-magnification TEM image for the folded edge of the MoS_2 film (different area in the same sample), where three layers of MoS_2 are clearly identified. Note that it is typical that the edge of free-hanging MoS_2 sheets folds on a TEM grid after TEM sample preparation process. Thus, the number of layers of the MoS_2 film can be resolved under top-view TEM. This method has been used for identifying number of graphene layers.[36] The TEM image in Figure 2c demonstrates that the MoS_2 film is highly crystalline. Figure 2d shows the selected area electron diffraction (SEAD) pattern taken with an aperture size (~160 nm) for the sample, as detailed in Figure S5. Figure S5d also shows the simulated SAED pattern with the MoS_2 lattice parameters: hexagonal $P6_3/mmc$ symmetry group, $a = b = 3.1$ Å, $C = 12.8$ Å. Note that the lattice constants we use here are obtained from our XRD data in Figure 3a, and these lattice

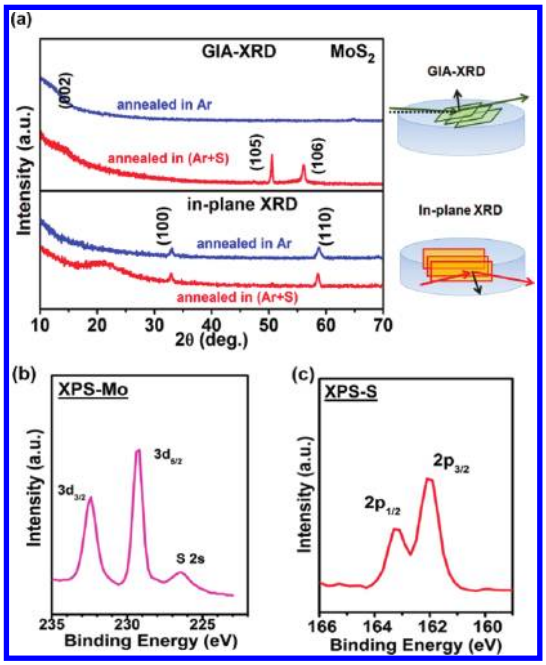

Figure 3. (a) Glancing incidence angle X-ray diffraction (GIA-XRD) and in-plane X-ray diffraction (in-plane XRD) patterns of the MoS_2 trilayers. (b, c) X-ray photoemission spectroscopy (XPS) measurements for the binding energies of Mo and S in the MoS_2 trilayers annealed with sulfur.

constants are in good agreement with the literature.[37] The distinct hexagonal lattice structure suggests that the film is highly crystalline MoS_2. It is noteworthy pointing out that the trilayer MoS_2 film synthesized on sapphire with sulfurization is actually polycrystalline, and the lateral size of the crystal domain is larger than 160 nm. We have also performed the other comparative measurements. Figures 2e,f and 2g–j respectively show the HRTEM and SAED results of the MoS_2 layers synthesized at 1000 °C with Ar annealing on sapphire and Ar + S annealing on SiO_2/Si. It is concluded that the domain size of MoS_2 layers grown on sapphire with sulfurization is clearly larger than the size of the films with only Ar annealing (~tens of nanometers). Moreover, the MoS_2 layers grown on a SiO_2/Si substrate with sulfurization exhibit inhomogenious crystal grain sizes. Some areas even show noncrystalline structures in HRTEM, as shown in Figure 2i,j. This observation suggests that the sapphire substrate is better than SiO_2.

To further reveal the effect of sulfur addition in the second annealing, the glancing incidence angle X-ray diffraction (GIA-XRD) and in-plane X-ray diffraction (in-plane XRD) were used to characterize the obtained MoS_2 trilayer. As shown in the schematic illustration in Figure 3a, the detector moves in perpendicular and parallel direction relative to sample surface in GIA-XRD and in-plane XRD, respectively. As a result, the diffraction signals respectively come from the in-plane contribution and the bulk except out-of-plane contribution. Figure 3a shows that the two pronounced peaks at $2\theta = 50.6°$ and 56.1°, assigned as the (105) and (106) reflections, respectively, can be clearly identified in GIA-XRD for the sample annealed with sulfur but not for that annealed in pure Ar. These two peaks are related to the diffraction from high-order (00l) planes. It is noted that a strong (002) peak is usually observed when the periodicity in c-axis (normal to the MoS_2 film plane) is present, but the (002) peak can hardly be detected on monolayer or few layer MoS_2.[7,13] Both samples show two peaks at $2\theta = 33.1°$ and 58.9° in the in-plane XRD measurements, assigned to (100) and (110) reflections, respectively. Note that all the observed peaks in in-plane and GIA-XRD can be reproduced well with the commonly accepted MoS_2 symmetry group: hexagonal $P6_3/mmc$.[37]

The addition of sulfur during the second annealing process clearly improved the crystallinity of MoS_2 thin layers. The X-ray photoemission spectroscopy (XPS) was used to measure the binding energies of Mo and S in the MoS_2 trilayers annealed with and without the presence of sulfur. Figure S6 displays the survey scans for these two films. The detailed binding energy profiles for Mo and S in both cases are similar, where we only show the spectra for the sample annealed with sulfur in Figure 3b,c. The Mo 3d shows two peaks at 229.3 and 232.5 eV, attributed to the doublet Mo $3d_{5/2}$ and Mo $3d_{3/2}$, respectively. The peaks, corresponding to the S $2p_{1/2}$ and S $2p_{3/2}$ orbital of divalent sulfide ions (S^{2-}), are observed at 163.3 and 162 eV. All these results are consistent with the reported values for MoS_2 crystal.[14,23] However, the XPS survey spectra in Figure S6 indicate that the oxygen content of the MoS_2 annealed in (Ar) is much higher. To further confirm this, TEM-based energy dispersive spectroscopy (TEM-EDS) is performed, and the results are shown in Table 1. The MoS_2 layers annealed in

Table 1. Results of TEM-EDS Analysis for MoS_2 Trilayers Annealed in (Ar) and in (Ar + S)

	atomic percentage		
annealing condition	Mo	S	O
(Ar)	22.7	55.1	22.2
(Ar + S)	33.2	60.1	6.7

(Ar) exhibit a high oxygen content (22.2 atomic %). The addition of sulfur in the second annealing seems to effectively reduce the oxygen content of MoS_2 films to ~6.7 atomic %. The oxygen species may come from the moisture absorbed on the MoS_2 surfaces and that unavoidably leaked into the chamber from the environments. These oxygen species are suspected to interrupt the crystal structure and degrade the electrical properties of the MoS_2. Our experiments suggest that, in addition to the increase of grain domain size as evidenced by

dx.doi.org/10.1021/nl2043612 | Nano Lett. 2012, 12, 1538–1544

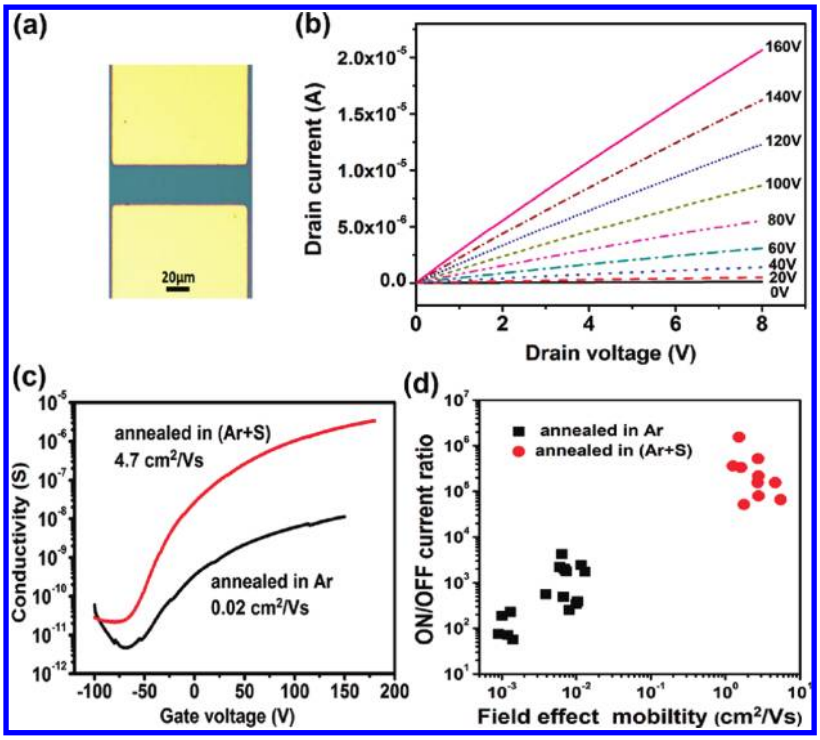

Figure 4. (a) Optical micrograph of the top view for the transistor device. (b) Output characteristics of the device made of trilayer MoS_2 synthesized on sapphire with (Ar +S). (c) The typical transfer curves (conductivity vs gate voltage V_g) for the devices fabricated using the MoS_2 trilayers annealed with and without sulfur. (d) Statistical comparison of the electron mobility and on/off current ratio for the devices fabricated using the MoS_2 trilayers annealed with and without sulfur.

TEM, the addition of sulfur can also help the removal of excess oxygen species in MoS_2 layers.

To evaluate the electrical performance of the MoS_2 thin layers, bottom-gate transistors were fabricated by evaporating Au/Ti electrodes directly on top of the MoS_2 trilayers on SiO_2/Si. Note that the MoS_2 films were grown on sapphire substrates and then transferred onto the freshly cleaned SiO_2/Si substrates since Figure S4 has demonstrated that the MoS_2 films grown on sapphire exhibited much better electron mobility values and on/off current ratios than those grown on SiO_2/Si substrates. The transfer process we adopted was similar to the method used for graphene,[38,39] and the details are described in the Supporting Information. In brief, the detachment of MoS_2 from the underlying sapphire substrate was done by partially etching the surface of sapphire with a NaOH solution by control of the etching time and NaOH concentration. Figure S7 displays the AFM images for the as-grown MoS_2 films on sapphire substrates and those after transferred onto SiO_2/Si substrates. In general, the thickness of the MoS_2 films grown on sapphire is quite uniform and the roughness of the large-area MoS_2 film is ~0.34 nm, and no wrinkles are observed (Figure S6b). After being transferred onto SiO_2/Si substrates, the film still maintained its initial lateral shape, but many wrinkles with a typical height ranging from 5 to 9 nm were formed. Figure 4a shows the top-view optical micrograph of the transistor device. Figure 4b displays the typical output characteristics (drain current I_d vs drain voltage V_d) for the MoS_2 device. Figure 4c compares the typical transfer curves (conductance vs gate voltage V_g) for the devices made from MoS_2 trilayers annealed with and without the presence of sulfur. It is observed that the sulfur annealing significantly increases the on/off current ratio from 2.4×10^3 to 1.6×10^5. Meanwhile, the field-effect electron mobility of the device annealed with sulfur is drastically enhanced from the order of 10^{-2} to 4.7 $cm^2/(V\ s)$. Note that the FET shows the typical n-typed behavior, consistent with the other reports.[3,4,35] The contact metal used in our devices is 80 nm Au with an adhesion layer Ti = 5 nm. The Fermi level of Ti (work function: 3.9−4.1 eV) is closer to the conduction band edge of MoS_2 (work function: 4.6−4.9 eV). Therefore, it is anticipated that the FET devices show n-typed behaviors and the threshold gate voltage are negative. The field-effect mobility of electrons was extracted based on the slope $\Delta I_d/\Delta V_g$ fitted to the linear regime of the transfer curves using the equation $\mu = (L/WC_{ox}V_d)(\Delta I_d/\Delta V_g)$, where L and W are the channel length and width and C_{ox} is the gate capacitance.[40] Figure 4d summarizes the statistical distribution of electron mobility values and on/off current ratios for the devices prepared from two types of MoS_2 films, where the electrical results agree well with the conclusion drawn from the spectroscopic measurements that the annealing with sulfur is necessary for obtaining high-quality MoS_2 thin layers. The effective field-effect mobility for the MoS_2 device can be up to 6 $cm^2/(V\ s)$ in ambient, comparable with previously reported data (0.1−10 $cm^2/(V\ s)$) for the micromechanically exfoliated MoS_2 sheets.[1,3,34,41]

Conclusions. In conclusion, we propose a two-step thermolysis process to synthesize large-area and highly crystalline MoS_2 thin layers. The addition of sulfur during the high-temperature annealing drastically enhances the crystallinity of MoS_2, as evidenced by various spectroscopic and microscopic characterizations including Raman, PL, XRD, TEM, and SAED. These MoS_2 thin layers can be easily transferred onto other arbitrary substrates. The transistor devices fabricated with MoS_2 thin layers in a bottom gate geometry exhibit n-type behaviors with the on/off current ratio ~10^5 and field-effect electron mobility up to 6 $cm^2/(V\ s)$,

dx.doi.org/10.1021/nl2043612 | Nano Lett. 2012, 12, 1538−1544

comparable with the devices prepared by the mechanically exfoliated MoS_2. The synthetic approach is simple and scalable.

■ ASSOCIATED CONTENT

Supporting Information

Experimental details; Figures S1−S7. This material is available free of charge via the Internet at http://pubs.acs.org.

■ AUTHOR INFORMATION

Corresponding Author

*E-mail: lanceli@gate.sinica.edu.tw.

Author Contributions

&These authors contribute equally.

Notes

The authors declare no competing financial interest.

■ ACKNOWLEDGMENTS

This research was supported by Academia Sinica (IAMS and Nano program), National Science Council Taiwan (NSC-99-2112-M-001-021-MY3 and 99-2738-M-001-001), and NCTU.

■ REFERENCES

(1) Novoselov, K. S.; Jiang, D.; Schedin, F.; Booth, T. J.; Khotkevich, V. V.; Morozov, S. V.; Geim, A. K. Two-dimensional atomic crystals. *Proc. Natl. Acad. Sci. U. S. A.* **2005**, *102*, 10451−10453.

(2) Rogers, J. A.; Lagally, M. G.; Nuzzo, R. G. Synthesis, assembly and applications of semiconductor nanomembranes. *Nature* **2011**, *447*, 45−53.

(3) Radisavljevic, B.; Radenovic, A.; Brivio, J.; Giacometti, V.; Kis, A. Single-layer MoS_2 transistors. *Nat. Nanotechnology* **2011**, *6*, 147−150.

(4) Radisavljevic, B.; Whitwick, M. B.; Kis, A. Integrated Circuits and Logic Operations Based on Single-Layer MoS_2. *ACS Nano* **2011**, *5*, 9934−9938.

(5) Splendiani, A.; Sun, L.; Zhang, Y.; Li, T.; Kim, J.; Chim, C.-Y.; Galli, G.; Wang, F. Emerging Photoluminescence in Monolayer MoS_2. *Nano Lett.* **2010**, *10*, 1271−1275.

(6) Aharon, E.; Albo, A.; Kalina, M.; Frey, G. L. Stable Blue Emission from a Polyfluorene/Layered-Compound Guest/Host Nanocomposite. *Adv. Funct. Mater.* **2006**, *16*, 980−986.

(7) Mak, K. F.; Lee, C.; Hone, J.; Shan, J.; Heinz, T. F. Atomically Thin MoS2: A New Direct-Gap Semiconductor. *Phys. Rev. Lett.* **2010**, *105*, 136805−1−4.

(8) Lee, C.; Yan, H.; Brus, L. E.; Heinz, T. F.; Hone, J.; Ryu, S. Anomalous Lattice Vibrations of Single- and Few-Layer MoS_2. *ACS Nano* **2010**, *4*, 2695−2700.

(9) Molina-Sánchez, A.; Wirtz, L. Phonons in single-layer and few-layer MoS_2 and WS_2. *Phys. Rev. B* **2011**, *84*, 155413−1−8.

(10) Korn, T.; Heydrich, S.; Hirmer, M.; Schmutzler, J.; Schüller, C. Low-temperature photocarrier dynamics in monolayer MoS_2. *Appl. Phys. Lett.* **2011**, *99*, 102109−1−3.

(11) Ghatak, S.; Pal, A. N.; Ghosh, A. Nature of Electronic States in Atomically Thin MoS_2 Field-Effect Transistors. *ACS Nano* **2011**, *5*, 7707−7712.

(12) Brivio, J; Alexander, D. T. L.; Kis, A. Ripples and Layers in Ultrathin MoS_2 Membranes. *Nano Lett.* **2011**, *11*, 5148−5153.

(13) Ramakrishna Matte, H. S. S.; Gomathi, A.; Manna, A. K.; Late, D. J.; Datta, R.; Pati, S. K.; Rao, C. N. R. MoS_2 and WS_2 Analogues of Graphene. *Angew. Chem., Int. Ed.* **2010**, *49*, 4059−4062.

(14) Rao, C. N. R. Nag, Angshuman Inorganic Analogues of Graphene. *Eur. J. Inorg. Chem.* **2010**, *27*, 4244−4250.

(15) Zhou, K. G.; Mao, N. N.; Wang, H. X.; Peng, Y.; Zhang, H. L. A mixed-solvent strategy for efficient exfoliation of inorganic graphene analogues. *Angew. Chem., Int. Ed.* **2011**, *50*, 10839−40.

(16) Zeng, Z. Y.; Yin, Z. Y.; Huang, X.; Li, H.; He, Q. Y.; Lu, G.; Boey, F.; Zhang, H. Single-Layer Semiconducting Nanosheets: High-Yield Preparation and Device Fabrication. *Angew. Chem., Int. Ed.* **2011**, *50*, 11093−11097.

(17) Joensen, Per; Frindt, R. F.; Morrison, S. Roy Single-layer MoS_2. *Mater. Res. Bull.* **1986**, *21*, 457−461.

(18) Ranjith Divigalpitiya, W. M.; Morrison, S. R.; Frindt, R. F. Thin oriented films of molybdenum disulphide. *Thin Solid Films* **1990**, *186*, 177−192.

(19) Divigalpitiya, W. M. R.; Frindt, R. F.; Morrison, S. R. Inclusion Systems of Organic Molecules in Restacked Single-Layer Molybdenum Disulfide. *Science* **1989**, *246*, 369−371.

(20) Eda, G.; Yamaguchi, H.; Voiry, D.; Fujita, T.; Chen, M.; Chhowalla, M. Photoluminescence from Chemically Exfoliated MoS_2. *Nano Lett.* **2011**, *11*, 5111−5116.

(21) Coleman, N.; Lotya, M.; et al. Two-Dimensional Nanosheets Produced by Liquid Exfoliation of Layered Materials. *Science* **2011**, *331*, 568−571.

(22) Li, Y.; Wang, H.; Xie, L.; Liang, Y.; Hong, G.; Dai, H. MoS_2 nanoparticles grown on graphene: an advanced catalyst for the hydrogen evolution reaction. *J. Am. Chem. Soc.* **2011**, *133*, 7296−9.

(23) Altavilla, C.; Sarno, M.; Ciambelli, P. A Novel Wet Chemistry Approach for the Synthesis of Hybrid 2D Free-Floating Single or Multilayer Nanosheets of MS_2@oleylamine (M=Mo, W). *Chem. Mater.* **2011**, *23*, 3879−3883.

(24) Lee, K.; Kim, H.-Y.; Lotya, M.; Coleman, J. N.; Kim, G.-T.; Duesberg, G. S. Electrical Characteristics of Molybdenum Disulfi de Flakes Produced by Liquid Exfoliation. *Adv. Mater.* **2011**, *23*, 4178−4182.

(25) Helveg, S.; Lauritsen, J. V.; Lægsgaard, E.; Stensgaard, I.; Nørskov, J. K.; Clausen, B. S.; Topsøe, H.; Besenbacher, F. Atomic-Scale Structure of Single-Layer MoS_2 Nanoclusters. *Phys. Rev. Lett.* **2000**, *84*, 951−954.

(26) Lauritsen, J. V.; Kibsgaard, J.; Helveg, S.; Topsoe, H.; Clausen, B. S.; Lagsgaard, E.; Besenbacher, F. Size-dependent structure of MoS_2 nanocrystals. *Nat. Nanotechnol.* **2007**, *2*, 53−58.

(27) Peng, Y.; Meng, Z.; Zhong, C.; Lu, J.; Yu, W.; Jia, Y.; Qian, Y. Hydrothermal Synthesis and Characterization of Single-Molecular-Layer MoS_2 and $MoSe_2$. *Chem. Lett.* **2001**, *8*, 772−773.

(28) Li, Q.; Newberg, J. T.; Walter, J. C.; Hemminger, J. C.; Penner, R. M. Polycrystalline Molybdenum Disulfide (2H-MoS2) Nano- and Microribbens by Electrochemicl/Chemical Synthesis. *Nano Lett.* **2004**, *4*, 277−281.

(29) Seo, J.; Jun, Y.; Park, S.; Nah, H.; Moon, T.; Park, B.; Kim, J.-G.; Kim, Y. J.; Cheon, J. Two-Dimensional Nanosheet Crystals. *Angew. Chem., Int. Ed.* **2007**, *46*, 8828−8831.

(30) Balendhran, S.; Ou, J. Z.; Bhaskaran, M.; Sriram, S.; Ippolito, S.; Vasic, Z.; Kats, E.; Bhargava, S.; Zhuiykov, S.; Kalantar-zadeh, K. Atomically thin layers of MoS2 via a two step thermal evaporation−exfoliation method. *Nanoscale* **2012**, *4*, 461−466.

(31) Seayad, A. M.; Antonelli, D. M. Recent Advances in Hydrogen Storage in Metal-Containing Inorganic Nanostructures and Related Materials. *Adv. Mater.* **2004**, *16*, 765−777.

(32) Pütz, J.; Aegerter, M. A. MoS_x Thin Films by Thermolysis of a Single-Source Precursor. *J. Sol-Gel Sci. Technol.* **2000**, *19*, 821−824.

(33) Pütz, J.; Aegerter, M. A. Liquid Film Deposition of Chalcogenide Thin Films. *J. Sol-Gel Sci. Technol.* **2003**, *26*, 807−811.

(34) Brito, J. L.; Ilija, M.; Hernfindez, P. Thermal and reductive decomposition of ammonium thiomolybdates. *Thermochim. Acta* **1995**, *256*, 325−338.

(35) Li, H.; Yin, Z. Y.; He, Q. Y.; Li, H.; Huang, X.; Lu, G.; Fam, D. W. H. A.; Tok, I. Y.; Zhang, Q.; Zhang, H. Fabrication of Single- and Multilayer MoS2 Film-Based Field Effect Transistors for Sensing NO at Room Temperature. *Small* **2012**, *8*, 63−67.

(36) Ferrari, A. C.; Meyer, J. C.; Scardaci, V.; Casiraghi, C.; Lazzeri, M.; Mauri, F.; Piscanec, S.; Jiang, D.; Novoselov, K. S.; Roth, S.; Geim, A. K. Raman Spectrum of Graphene and Graphene Layers. *Phys. Rev. Lett.* **2006**, *97*, 187401−1−4.

(37) Symmetry group: $P6_3/mmc$; lattice parameters $a = b = 3.16$ Å and $c = 12.295$ Å from: Hulliger, F. In *Structural Chemistry for Layer-Type Phases*; Levy, F., Ed.; Riedel: Dordrecht, 1976.

(38) Su, C.-Y.; Fu, D.; Lu, A.-Y.; Liu, K.-K.; Xu, Y.; Juang, J.-Y.; Li, L.-J. Transfer printing of graphene strip from the graphene grown on copper wires. *Nanotechnology* **2011**, *22*, 185309−1−6.
(39) Cheng, Z.; Zhou, Q.; Wang, C.; Li, Q.; Wang, C.; Fang, Y. Toward Intrinsic Graphene Surfaces: A Systematic Study on Thermal Annealing and Wet-Chemical Treatment of SiO_2-Supported Graphene Devices. *Nano Lett.* **2011**, *11*, 767−771.
(40) Lee, C. W.; Weng, C.-H.; Wei, L.; Chen, Y.; Chan-Park, M. B.; Tsai, C.-H.; Leou, K.-C.; Poa, C. H. P.; Wang, J.; Li, L.-J. Toward High-Performance Solution-Processed Carbon Nanotube Network Transistors by Removing Nanotube Bundles. *J. Phys. Chem. C* **2008**, *112*, 12089−12091.
(41) Yoon, Y.; Ganapathi, K.; Salahuddin, S. How Good Can Monolayer MoS_2 Transistors Be? *Nano Lett.* **2011**, *11*, 3768−3773.